Available online at **www.joac.info**

ISSN: 2278-1862

Journal of Applicable Chemistry

2018, 7 (4): 905-918

(International Peer Reviewed Journal)

Synthesis, Characterization, DNA binding, Anti-Bacterial and VEGF-C Growth Factor Docking Studies of New Cu(II), Ni(II) and Co(II) Complexes

A. Anjaneyulu, K. Kamalaker Reddy, J. Sunitha, M. Sayaji Rao*

Department of Chemistry, Osmania University, Hyderabad, 500007, Telangana, **INDIA**

Email: raosayaji@yahoo.co.in

Accepted on

ABSTRACT

*Three mono nuclear [Cu(ibpc)$_2$] (**1**),[Ni(ibpc)$_3$](**2**) and [Co(ibpc)$_2$](**3**)complexes were synthesized and characterized utilizing various spectroanalytical techniques viz., ESI-Mass, UV, IR, TGA,SEM-EDX, magnetic moment and molar conductance experiments. The complexes were screened for their DNA interaction and antibacterial activities. Docking interactions of complexes with VEGF-C growth factor were also performed using Accelry's discovery studio 2.5. All the complexes bound to DNA molecule in an intercalative mode and exhibited an average activity against selected gram negative and gram positive bacterial strains. The Binding ability of complexes with DNA was found to be in the order **2**>**1**>**3** with K_b values $3.21\times10^3M^{-1}$, $2.97\times10^3M^{-1}$ and $1.11\times10^3M^{-1}$ for **2**, **1** and **3** respectively. Complex **1** showed good binding affinity with VEGF-C growth factor. The observed low molar conductance values indicate the non-electrolytic nature of the complexes. Ibpc=2-(4-iso propylbenzylidene)-N-phenylhydrazinecarbothioamide.*

Graphical Abstract

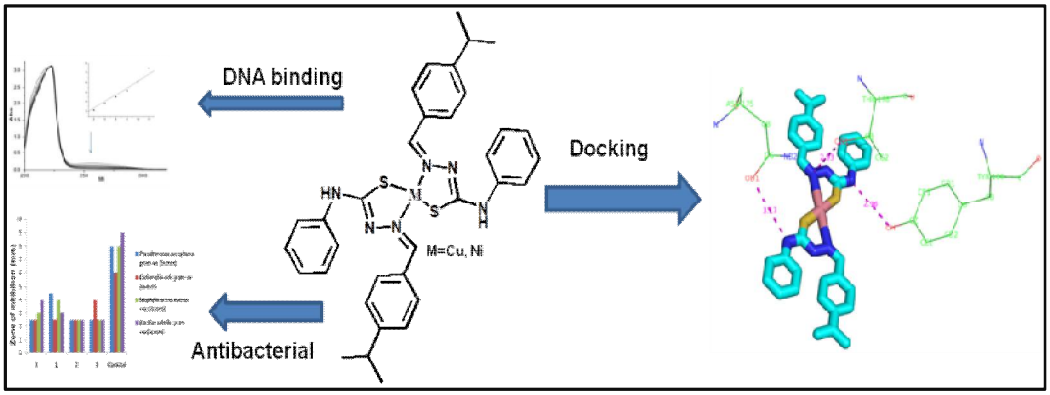

Keywords: Mono nuclear complexes, Docking, Intercalation, Antibacterial activity, Non-electrolytic nature.

INTRODUCTION

Interaction of metalloreagents with DNA molecule is widely studied in recent times [1, 2]. Yet there is a need for the synthesis of efficient metalloreagents for promising biological activities. In the present investigation we have employed Schiff bases derived from substituted thiosemicarbazide and cuminaldehyde to coordinate with Cu(II), Ni(II) and Co(II)ions.Cu(II) is the extensively studied and most prominent transition metal ion with its metal complexes in treating many diseases [3, 4]. Cobalt is a biological trace element which helps in the production of RBC and proper functioning of nervous system.Although Nickel is toxic in low doses, its complexes were also used to explore possible biological activities [5]. Metal complexes derived from thiosemicarbazones are known to possess high biological activities [6-10]. Also thiosemicarbazones are known to inhibit RDR (Rhibonucleotide Diphosphate Reductase) enzyme which plays a key role in the synthesis of DNA precursors [11]. In view of this, an attempt has been made to synthesize thiosemicarbazone based metal complexes and initiated few biological studies. Hypoxia is a common condition in cervix cancer and is associated with lymph node metastasis [12]. Vascular endothelial growth factor C has been identified as major regulator of the lymphatic vessels (lymphangiogenesis). Many of human cancers such as prostate, cervix, colorectal and lung cancers found to have the expression of VEGF-C in lymphatic node metastasis [13]. Tumor tissues often suffer from hypoxia, a condition in which upregulation of VEGF-C is observed [14]. Interfering with VEGF-C signaling pathways is an useful clinical strategy in the treatment of lymphatic metastasis [15]. Molecular docking is a reliable tool for drug design prior to the examination of a drug's potential in *in vitro* conditions. Hence, we have docked the ligands into active site residues of VEGF-C for estimating their binding ability. The results showed good binding ability of complexes with VEGF-C growth factor, which is an indication for their application in cancer therapy.

MATERIALS AND METHODS

4-isopropylbenzaldehyde, 4-phenylthiosemicarbazide and hydrated metal chlorides were purchased from Sigma Aldrich and were used without further purification. All other chemicals and solvents of analytical reagent grade were purchased from commercial sources and were used without further purification. Distilled water was employed to prepare buffer solutions. Absorption titrations were carried out in buffer solution of 5 mM Tris-HCl/50 mM NaCl. Elemental analysis was obtained using Heraeus CarlovErba 1108 elemental analyzer. IR spectra were recorded in KBr pellets using a Perkin Elmer FT-IR spectrophotometer in the range of 4000–350 cm^{-1}. UV/Vis reflectance spectra for complex (**2**) were recorded on UV-VIS-NIR spectrophotometer (UV 3600). Magnetic susceptibility was recorded at room temperature on a Faraday balance (CAHN-7600) using $Hg[Co(NCS)_4]$ as the standard. Diamagnetic corrections were made by using Pascal's constant [16]. The molar conductivity was measured on a Digison digital conductivity bridge (model: DI-909) with a dip type cell. Docking studies with VEGF-C protein were performed in Accelry's discovery studio 2.5.

Synthesis

Synthesis of ligand: 1mmol (0.148 gm) ethanolic solution of cuminaldehyde was added to 1mmol (0.167 gm) ethanolic solution of 4-phenyl thiosemicarbazidein hot condition and refluxed for 4 h. A color less liquid obtained was dried over vacuum and the compound was purified over silica gel using 1% ethylacetate-hexane solution as elutant.

Synthesis of complexes 1, 2 and 3: 1 mmol aqueous solutions of $CuCl_2.H_2O$ (0.170 gm), $NiCl_2.6H_20$ (0.237 gm) and $CoCl_2.6H_2O$ (0.238 gm) were slowly added to the hot ethanolic solutions of 2 mmol (0.594 gm) thiosemicarbazone ligand. After refluxing the reaction mixtures for four hours, grey (for **1**), light green (for **2**) and dark pink (for **3**) colored precipitates were formed. Precipitates were washed several times with hexane and kept in vacuum for 24 h for drying.

Analytical data

Data for 1: Yield: 75%, M.P. 200°C, IR (KBr Phase): ϑ_{max}/cm^{-1}: 3269, 3122, 1597, 831, 443, 372, m/z: 657 $[M+H]^+$, μ_{eff}: 1.80 BM.$\Lambda_M(\Omega^{-1}\ cm^2\ M^{-1})\ 10^{-3}$ M solution at room temperature (DMF) 21; Elemental analysis: Calculated for $C_{34}H_{36}CuN_6S_2$ = C, 62.22; H, 5.53; N, 12.80; found; C, 61.07; H, 5.21; N, 12.56

Data for 2: Yield: 87%, M.P. 196°C, IR (KBr Phase): ϑ_{max}/cm^{-1}: 3398, 3215, 1602, 822, 432, 345, m/z: 949 $[M+H]^+$, UV/Vis Solid reflectance: 640 nm, μ_{eff}: 2.90 BM.: $\Lambda_M(\Omega^{-1}\ cm^2\ M^{-1})\ 10^{-3}$M solution at room temperature (DMF) 23;Elemental analysis: Calculated for $C_{51}H_{54}CNiN_9S_3$ = C, 64.29; H, 5.71; N, 13.23; found; C, 62.33; H, 5.62; N, 12.95

Data for 3: Yield: 62%, M.P. 170°C, IR (KBr Phase): ϑ_{max}/cm^{-1}: 3385, 3049, 1599, 823, 493, 381, m/z: 651 $[M+H]^+$, μ_{eff}: 3.98 BM.Λ_M $(\Omega^{-1}\ cm^2\ M^{-1})\ 10^{-3}$ M solution at room temperature (DMF) 19; Elemental analysis: Calculated for $C_{34}H_{36}CoN_6S_2$ = C, 62.22; H, 5.53; N, 12.80; found; C, 62.13; H, 5.17; N, 11.73

DNA binding

Preparation of stock solution: Concentrated CT-DNA stock solution was prepared in 5 mM Tris-HCl/50 mM NaCl in H_2O at pH 7.5 and the concentration of DNA solution was determined by UV absorbance at 260 nm. The molar absorption coefficient was taken as $6600M^{-1}cm^{-1}$ [17]. Solution of CT-DNA in 5 mM Tris -HCl/50 mM NaCl (Tris buffer; PH=7.5) gave a ratio of UV absorption at 260 and 280 nm, $A_{260}/A_{280}$of ca.1.8-1.9, indicating that the DNA was sufficiently free of protein [18]. All stock solutions were stored at 4°C and were used within 4 days. The concentration of EB was determined spectrophotometrically at 480 nm ($\varepsilon=M^{-1}cm^{-1}$) [19]. Binding experiments were done in Tris buffer with 10^{-3} M concentration of complexes in methanol.

Absorption Spectra: Absorption spectra were recorded on Jasco V-530 UV/VIS spectrometer using 1-cm quartz micro-cuvettes. Absorption titrations were performed by keeping the concentration of the complexes **1**, **2** and **3**at 10 µM and by varying the CT-DNA concentration from 0-10µM. DNA blank was placed in the reference cell so as to offset any absorbance due to DNA at measured wavelength. The binding constant (K_b) were determined from the spectroscopic titration data using the following equation [20].

$$[DNA]/(\varepsilon_a-\varepsilon_f)=[DNA]/(\varepsilon_b-\varepsilon_f)+1/K_b(\varepsilon_b-\varepsilon_f) \quad .....(1)$$

The apparent extinction coefficient (ε_a) was obtained by calculating $A_{obs}/[M]$. The terms ε_f and $\varepsilon_b$correspond to the extinction coefficients of free (unbound) and the fully bound complexes, respectively. A plot of $[DNA]/(\varepsilon_a-\varepsilon_f)$ vs [DNA] will give a slope $1/(\varepsilon_b-\varepsilon_f)$ and an intercept $1/K_b(\varepsilon_b-\varepsilon_f)$.$K_b$ is the ratio of the slope and the intercept.

Viscosity: Viscometric titrations to measure flow times were performed with an Ostwald viscometer at room temperature. The concentration of DNA was kept constant at 200 μM and complex concentrations were varied from 0-120 μM. Flow times were measured with a digital timer, and each measurement was repeated three times and an average flow time was calculated. Data were presented as $(\eta/\eta_0)^{1/3}$ vs [Complex]/[DNA], where η is the viscosity of DNA in the presence of complex and η_0 is viscosity of DNA alone. Viscosity values were calculated from the observed flow time of DNA containing solutions (t) corrected for that buffer alone(5 mM Tris-HCl/50 mM NaCl) (t_0),$\eta=(t-t_0)$.

Antibacterial activity: The metal complexes (**1-3**)were screened for their*in vitro* antibacterial activity against gram positive and gram negative bacterial strains by cup-plate agar diffusion method at different concentrations (0.5, 1mg mL^{-1}) [21, 22]. *Pseudomonas aeruginosa* (gram-negative), *Escherichia coli* (*E. coli*) (gram-negative), *Bacillus subtilis* (gram-positive) and *Staphylococcus*

aureus (gram-positive) were obtained from Microbial Type Culture Collection –MTCC. The bacterial strains were autoclaved in LB broth media and incubated over night at 37°C in shaker for Bacterial growth. From that 0.3 mL of bacterial culture was taken and inoculated by using spreader on freshly prepared autoclaved agar plates i.e., Petri dishes. After drying the plates, 5 mm sample discs which dissolved in DMSO solvent were kept on microbial plate along with positive controls NX (Norfloxacin) for *Staphylococcus, Pseudomonas* and OF (Ofloxacin) for *Bacillus* and *E.coli*. and incubated over night at 37ºC in BOD incubator. After overnight incubation zone of inhibition was measured by measuring scale.

Molecular docking: Docking interactions between ligands (**1-3**) and VEGF-C growth factor were estimated by utilizing Accelry's Discovery studio 2.5. The 3D structure of target protein was retrieved from protein data bank (RCSB PDB ID: 2X1W). All the essential steps, such as removal of water molecules, addition of hydrogen atoms for correct ionization and tautomeric states and correction of missing loops were undertaken for the preparation of clean protein structure. 2D structures of ligands were drawn using chemdraw and Ligfit search algorithm was used to dock the ligands into active pocket of target protein. Accelry's CHARMm force field was used to obtain energy minimized conformer of protein with a maximum number of 1000 steps at 0.01 RMS gradient. The scoring functions were utilized to predict the binding affinity of ligands with target protein [23].

RESULTS AND DISCUSSION

The schematic representation for the synthesis of complexes (**1-3**) was depicted in scheme 1. All complexes were soluble in DMSO, DMF and insoluble in H_2O. The compounds were stable in solid phase and solution phase. They were not absorbing any water content from atmosphere, which proves their non-hygroscopic nature. All attempts to obtain single crystals for compounds were failed. The observed low molar conductance values confirm their non-electrolytic nature. All the Complexes were thoroughly characterized and obtained spectroanalytical data is in good agreement with the molecular formulae of corresponding complexes.

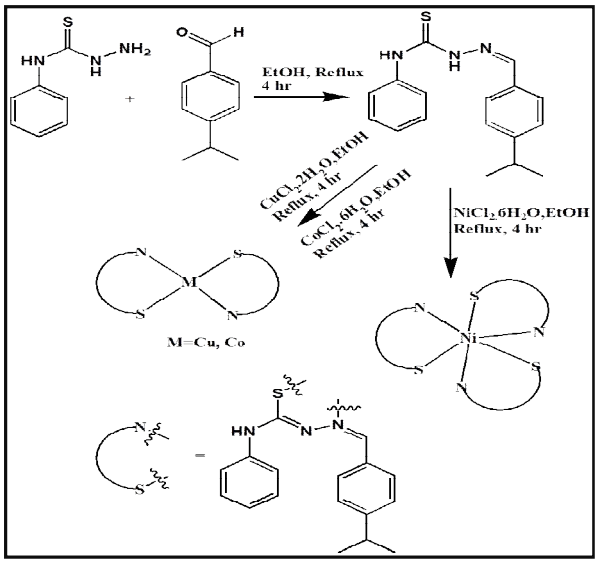

Scheme 1. Schematic representation of synthetic route for the complexes **1-3.**

Mass spectra: The mass spectra of the synthesized complexes were recorded in ESI positive ion mode.The base peaks located at m/z 657 $[M+H]^+$(**1**) (Fig.1), m/z 949 $[M]^+$ (**2**) (Fig.2) and m/z 651 $[M]^+$(**3**) (Fig.3) proves the complexation of ligand with metal ion.

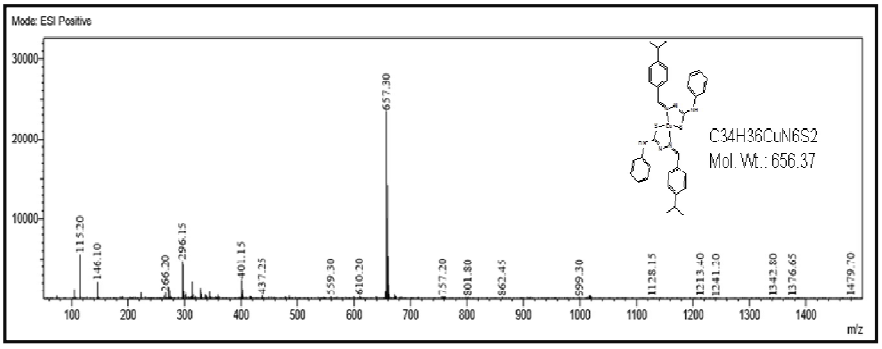

Figure 1. ESI-Mass spectra of complex **1.**

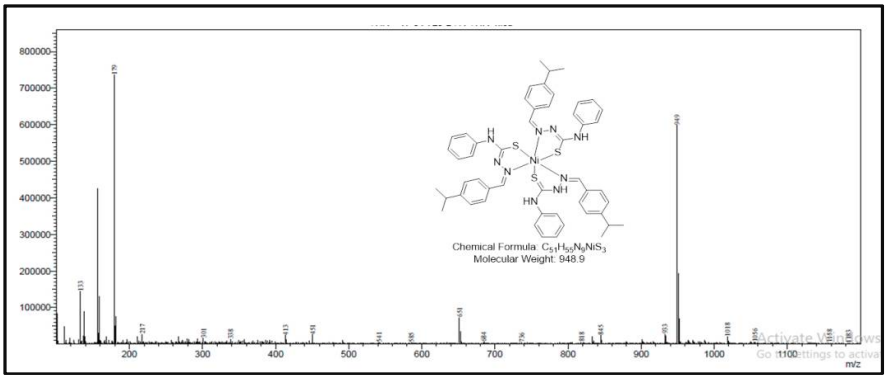

Figure 2. ESI-Mass spectra of complex **2**

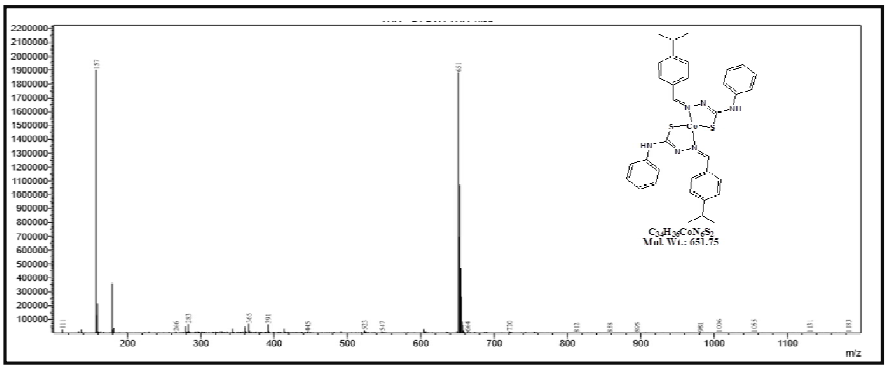

Figure 3. ESI-Mass spectra of complex **3.**

IR Spectra: The IR frequencies were used to further elucidate the structures of synthesized compounds [24]. Two sharp bands observed in the region 3320-3140 cm^{-1} were assigned to –NH/NH-Ph vibrational modes. The IR spectra of free ligand exhibited an intense and sharp peak at 1595 cm^{-1} which is assignable to azomethine (C=N) group. Upon complexation, the sharp bandfor free ligand was shifted to 1597 cm^{-1} (**1**), 1601 cm^{-1}(**2**) and 1598 cm^{-1}(**3**) respectively, indicating the chelation of ligand to corresponding metal ions. The IR stretching frequency of C=S at 619 cm^{-1} for free ligand is absent in metal complexes, indicating the chelation of enolic sulphur atom [25]. The non ligand peaks corresponding to M-N were located at 443 cm^{-1}, 432 cm^{-1} and 493cm^{-1} for **1-3** respectively indicating coordination of N atom of free ligand to metal ion. Other non ligand peaks corresponding to the stretching frequencies of M-S were located at 372 cm^{-1} (for **1**), 345 cm^{-1} (**2**) and 381 cm^{-1}(**3**), which is an indication for the chelation enolic sulphur to metal ion. The IR spectral details are represented in fig. 4 (for **2**), fig. 5 (**3**). IR spectral details of complex **1** are presented in fig. S1.

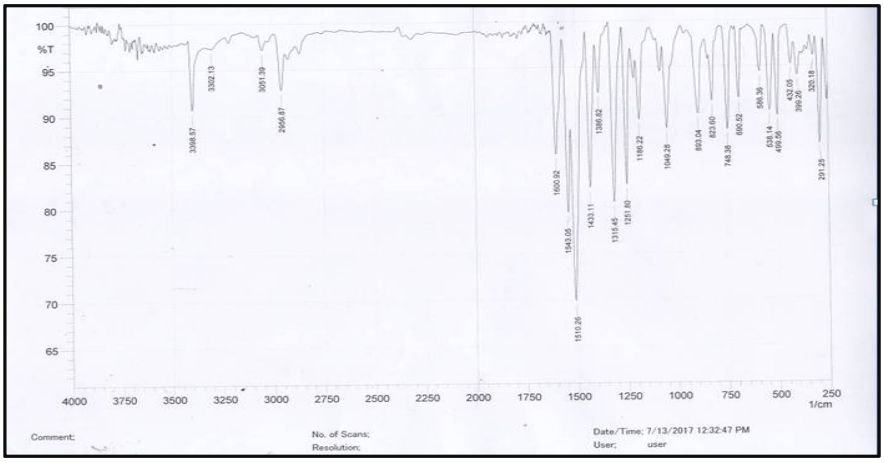

Figure 4. IR spectra of complex **2.**

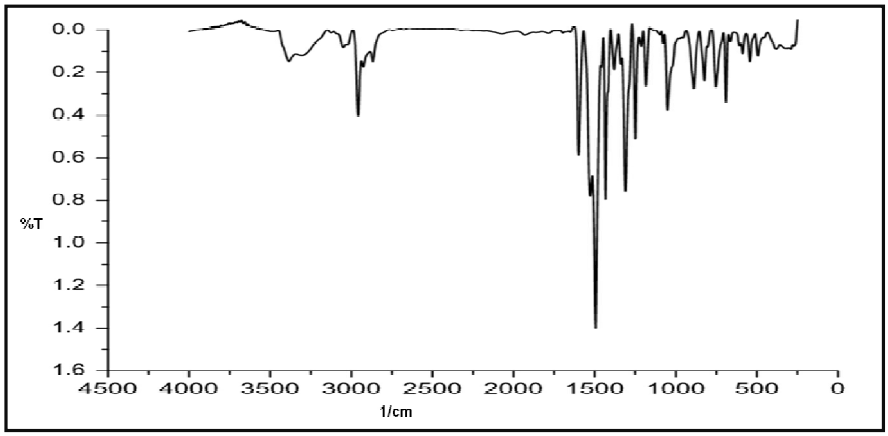

Figure 5. IR spectra of complex **3.**

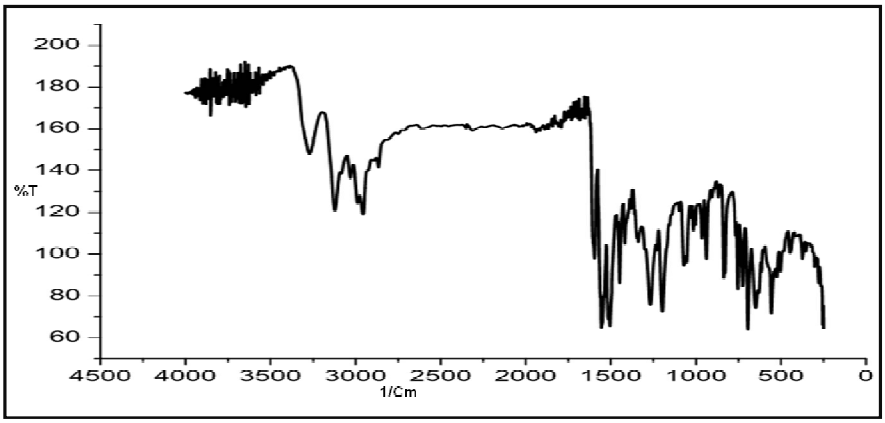

Figure S1.IR spectra of complex **1.**

UV-Vis Spectra: For complex **2**, the observed band location is typical of octahedral geometry. The solid reflectance spectra of **2** showed a clear broad band located at 640 nm which is consistent with $^3T_{1g} \rightarrow {}^3A_{2g}$ transition (Fig. 6) [**26**]. This transition confirms octahedral geometry around Ni (II) ion.

Charge transfer bands located at 230 nm and 320 nm correspond to n-π* and π-π* transitions, respectively.

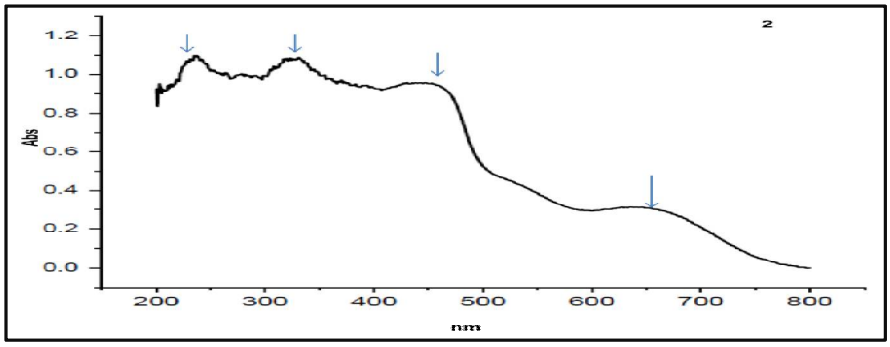

Figure 6. Solid reflectance spectra of complex **2.**

SEM-EDX: The surface morphology images were obtained using scanning electron microscope (SEM) attached with an EDX spectrometer. The EDX data revealed high stoichiometric formation of complexes. SEM images were represented in fig. 7 and EDX plots are presented in fig. S2.

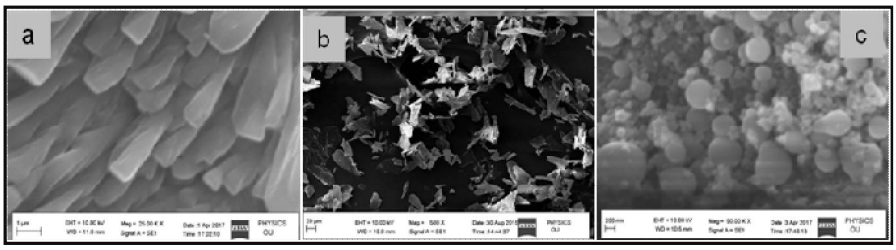

Figure 7. SEM images of complexes **1**(a), **2**(b) and **3**(c).

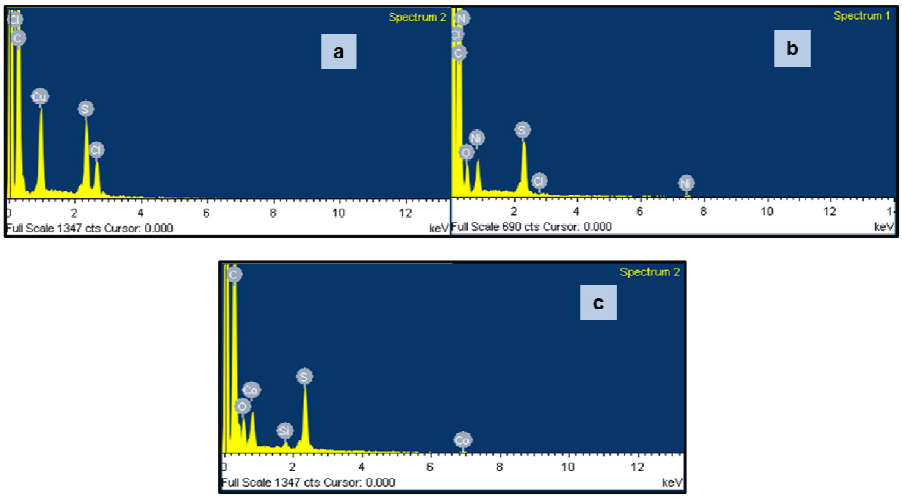

Figure S2. EDX Plots of metal complexes**1-3**

Magnetic moment: The magnetic moment of the complexes were found to be 1.80, 2.90, 3.98, suggesting the paramagnetic nature of the complexes with one, two , three unpaired electrons for **1**, **2** and **3** respectively.

Thermo Gravimetric Analysis: The presence of lattice and coordinated water molecules was investigated by TGA. The thermal decomposition curves of complexes **1-3** were presented in fig. 8

(for **1**), fig. S3(**2**) and fig. S4(**3**). Complexes **1-3** did not show any weight loss upto150 corresponding to water molecules. This clearly indicates that no water molecules were present in the vicinity of the complexes **1-3** [27].

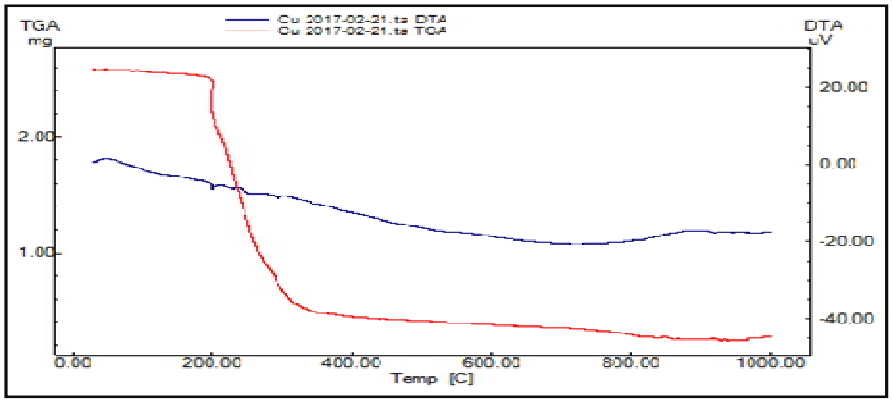

Figure 8. TGA spectra of complex **1.**

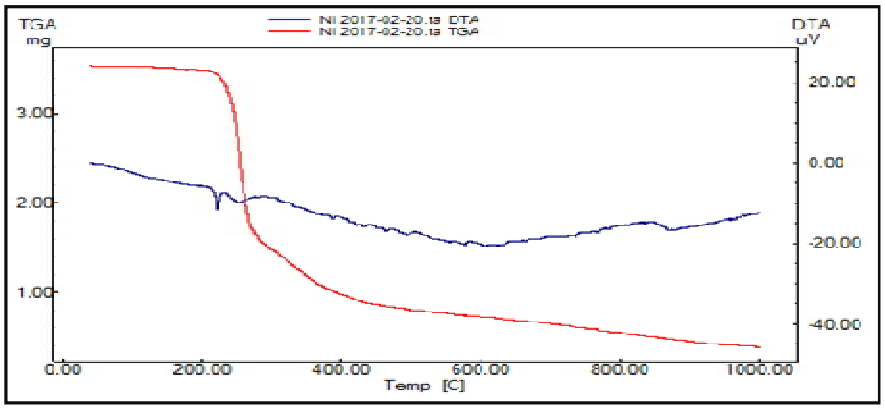

Figure S3. TGA spectra of complex **2.**

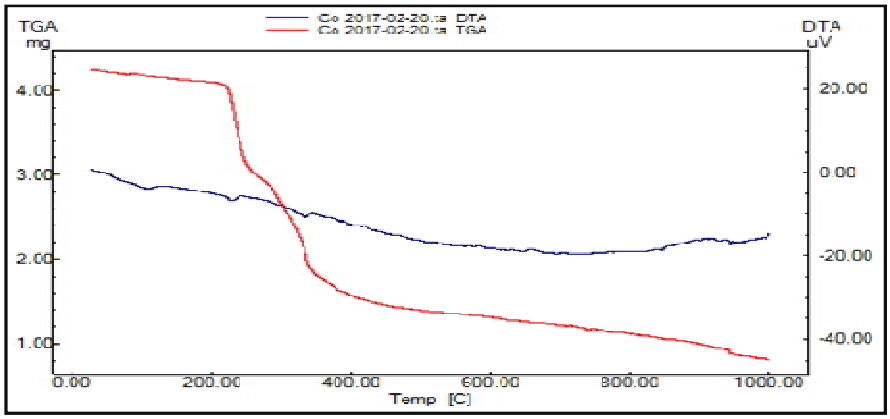

Figure S4. TGA spectra of complex **3.**

DNA binding: The mode of binding of complexes **1-3** to CT-DNA were studied by the following techniques.

Absorption spectrometry: The absorption patterns of complexes **1-3** in the absence and presence of CT-DNA were shown in fig. 9 (for **2**), fig. S5(**1**) and fig. S6(**3**). The addition of increasing amounts of DNA to the complexes resulted in bathochromic and hypochromic shifts.Hypochromism is a consequence of intercalative mode of binding involving a strong stacking interaction between an aromatic chromophore and the base pairs of DNA [28, 29].After intercalation with base pairs of DNA the π* orbitals of complex further interacts with the π orbital of base pairs,thuslowers the π-π* transition energy and resulting in bathochromism [30]. The intrinsic binding constants were found to be 2.97×10^3 M^{-1}, 3.21×10^3 M^{-1} and $1.11\times10^3M^{-1}$ for complexes **1-3** respectively.

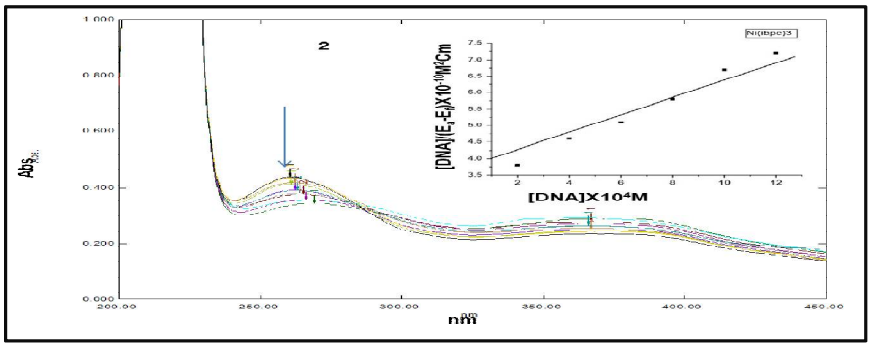

Figure 9. Electronic absorption spectra of Ni (II) complex (**2**) in the absence and presence of increasing amount of CT-DNA. Conditions: [**2**]=10μM; CT-DNA=0-10μM. Arrow shows the absorbance changes upon increasing DNA concentration. Insets: linear plot for the calculation of intrinsic binding constant (K_b).

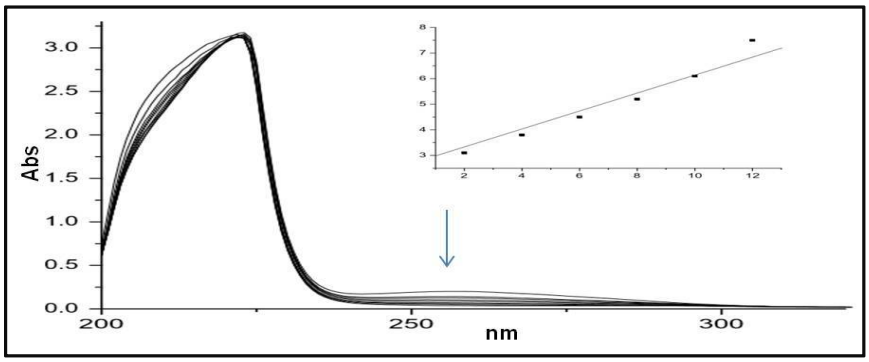

Figure S5. Electronic absorption spectra of Cu (II) complex (**1**) in the absence and presence of increasing amount of CT-DNA. Conditions: [**1**]=10μM; CT-DNA=0-10μM. Arrow shows the absorbance changes upon increasing DNA concentration. Insets: linear plot for the calculation of intrinsic binding constant (K_b).

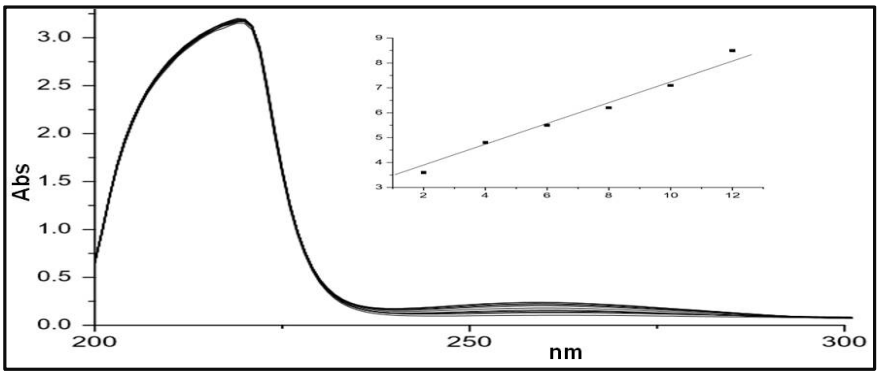

Figure S6. Electronic absorption spectra of Co (II) complex (**3**) in the absence and presence of increasing amount of CT-DNA. Conditions: [**3**]=10μM; CT-DNA=0-10μM. Arrow shows the absorbance changes upon increasing DNA concentration. Insets: linear plot for the calculation of intrinsic binding constant (K_b)

Viscosity: The intercalative mode of binding was further supported by viscosity experiment. The relative viscosity of CT-DNA solutions is known to increase when DNA interacts with intercalative binding substrates [31]. The effect of **1-3** complexes on the viscosity of DNA at room temperature was depicted in Fig. 10.As can be seen from figure the viscosity of DNA is increased with increasing amount of the complexes. This behavior is consistent with other intercalators such as ethedium bromide. This clearly indicates that all complexes intercalate between adjacent DNA base pairs causing an extension in the helix there by increasing the viscosity of DNA [32, 33].

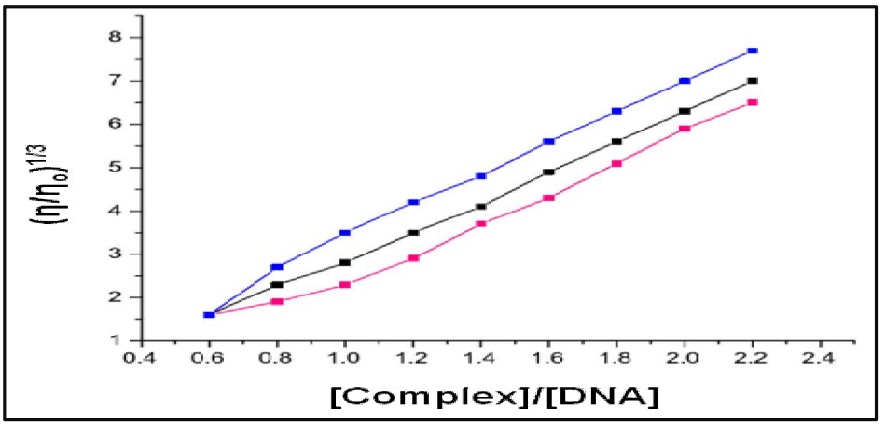

Figure 10. Effect of increasing amount of complexes **1** (blue), **2** (black) and **3** (pink) on the relative viscosities of CT-DNA at room temperature in Tris HCl buffer 5mM. Conditions: [DNA]/200µM; [**1-3**]0-120µM.

Antibacterial activities: The complexes(**1-3**) were screened for their antibacterial activities.Two gram positive bacterial strains (*Staphylococcus aureus, Bacillus subtilis*) and two gram negative bacterial strains (*Pseudomonas aeruginosa, Escherichia coli* (*E. coli*)) were used in this investigation. As shown in the fig. 11 and table 1, it is clear that the copper complex(**1**) has higher activity against pseudomonas and staphylococcus bacterial strains, which may be attributed to its higher permeable nature [34, 35]. Despite the resistance of gram negative strains to complexes, the antibacterial studies demonstrated higher activity against gram positive strains. Though the activity of complexes is less as compared to the controls, they could be further developed as potential antibacterial agents by introducing suitable functional groups on to the ligand moiety.

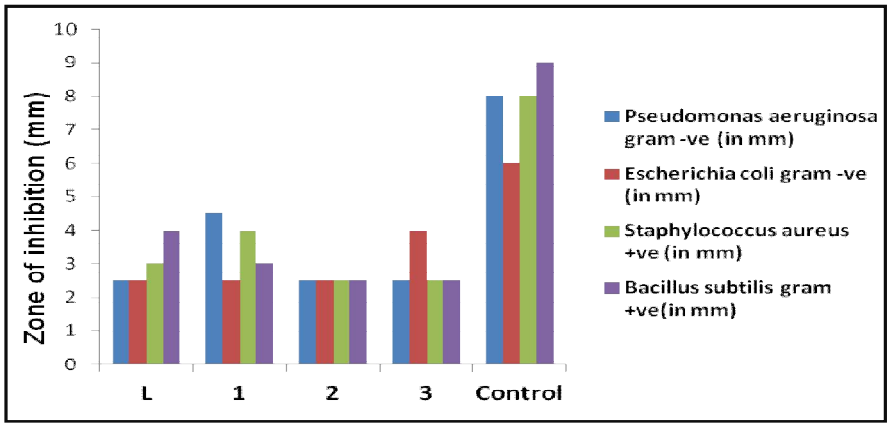

Figure 11. BAR diagram showing antibacterial activity of complexes **1-3** against selected bacterial strains.

Table 1. Zone of inhibition values in mm.

Compound	*Pseudomonas aeruginosa* (gram -ve)	*Escherichia coli* (gram -ve)	*Staphylococcus aureus* (gram +ve)	*Bacillus subtilis* (gram +ve)
L	2.5	2.5	3	4
1	4.5	2.5	4	3
2	2.5	2.5	2.5	2.5
3	2.5	4	2.5	2.5
Control	8	6	8	9

Molecular docking: The Ligfit module from Discovery studio was utilized to carry out the molecular docking of ligands with active site residues of VEGF-C protein (Fig. 12). The binding affinity of ligands with target protein was ranked by Ligfit scores. As can be seen from table 2, complex **1** exhibited higher docking score and hydrogen bonds which indicate high binding affinity with receptor protein. The binding ability of complexes with receptor protein follows the order **1**>**2**>**3**. Complex **1** may have better utility in drug design over complex **2** and **3** as it is having higher binding affinity.

Table 2. Docking energy of ligands (**1-3**) in the active site pocket of VEGF-C growth factor (PDB ID: 2X1W).

Ligand Name	Interacting Residues		Distance (A^o)	Docking Energy (kcal mol^{-1})
	Ligand	Receptor (2X1W)		
1	NH	THR178 - OG1	2.87	-91.256
	NH	TYR180 - O	2.96	
2	NH	ASN175 – OD1	2.85	-90.021
	NH	THR178 – OG1	3.03	
3	NH	THR178-OG1	2.93	-90.679
	NH	TYR180-O	2.96	
	NH	ASN175-OD1	3.17	

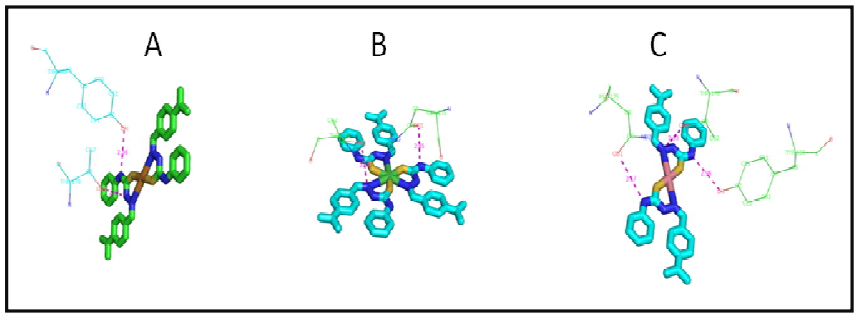

Figure 12. Interactions of ligands **1**(A), **2**(B) and **3**(C) in the active site pocket of VEGF-C growth factor (PDB ID: 2X1W).

APPLICATION

Above results suggest that the complexes could be used as therapeutic agents in treating cancer because of their DNA binding ability and VEGF-C growth factor binding affinity.

CONCLUSIONS

In the present study, three mono nuclear complexes were synthesized and structure elucidated by various spectroscopic techniques. The geometry of Cu(II) and Co(II) was found to be Square planar and that of Ni(II) was octahedral. The compounds showed good DNA binding affinity and moderate

activity against selected gram positive bacterial strains. Docking studies revealed their binding affinity with VEGF-C protein.

ACKNOWLEDGMENT

The authors are grateful to University Grants Commission, INDIA for financial assistance.

REFERENCES

[1]. P. R .Reddy, S. Rajeshwar, B. Satyanarayana, synthesis characterization of new Cu(II) Schiff base and 1,10 phenanthroline complexes and study of their bio properties, *J. Photochem. Photobiol B: Biology.*, **2016**, 160, 217-224.
[2]. M. Sunitha, B. Anupama. B. Usaiah, C. Gyanakumari, synthesis, characterization, DNA binding and cleavage studies of mixed- ligand copper (II) complexes, *Arab. J. Chem.,***2017**, 10, S3367-S3374.
[3]. L. J. K. Berner, J. M. Zaleski, metal complex DNA interactions: From Transcription to photo activated cleavage, *Curr. Opin. Chem. Biol.*, **2005**, 9, 135-144.
[4]. J. T. Wan, Q. Xia, H. X. Zheng, H. Y. Chen, H. Chao, Z. W. Mao, L. N. Ji, An effective approach to artificial nucleases using copper (II) complexes bearing nucleobases, *Dalton Trans.*, **2010**, 39, 2128-2136.
[5]. S. Chandra, M. Tyagi, P. K. sharma, Spectroscopic and biological approach of Ni (II) and Cu (II) complexes of 2-pyridinecarboxaldehyde thiosemicarbazone, *Spectrochim. acta A*., **2008**, 69, 816-821.
[6]. W. Hernandez, J. Paz, A. Vaisberg, E. Spodine, R. Richter, L. Beyer. Synthesis and characterization, and In Vitro cytotoxic activities of benzaldehyde thiosemicarbazone derivatives and their palladium (II) and Platinum (II) Complexes against Various Human Tumor Cell Lines, *Bioinorg. Chem. appl.*, **2008**, 2008, 1-9.
[7]. S. Bjelogrlic, T. Todorovic, A. Bacchi, M. Zec, D.Sladic, T. S.Rajic, D Radulovic, G Pelizzi, Kandelkovic, Synthesis, structure and Characterization of novel Cd(II) and Zn(II) complexes with the condensation product of 2-formylpyridine and selenosemicarbazide antiproliferative activity of the synthesized complexes and related selenosemicarbazone complexes, *J. Inorg. Biochem.*, **2010**, 104, 673-682.
[8]. K. Alomar, A. Landreau, M. Kempf, M. A. Khan, M. allain, G. Bouet, synthesis ,crystal structure, characterization of Zinc (II), Cadmium (II) complexes with 3-thiophene aldehyde thisemicarbazone (3TTSCH), biological activities of 3TTSCH and its Complexes. *J. Inorg. Biochem.*, **2010**, 104, 397-404.
[9]. T. P. Stanojkovic, D. K. Demertzi, A.Primikyri, I. G. Santos, A. Castineiras, Z. Juranic, M. A Demertzis, Zinc(II) complexes of 2-acetyl pyridine 1-(4-fluorophenyl)-piperazinyl thiosemicarbazone: Synthesis, spectroscopic study and crystal structures – Potential anticancer drugs, *J. Inorg. Biochem*., **2010**, 104, 467-476.
[10]. F. R. Pavan, P. I. D. S. Maia, S. R. A. Leite, V. M. Deflon,A. A Batista, D. N. Sato, S. G. Franz blau, C. Q. F. Leite, Thiosemicarbazones, semicarbazones, dithiocarbazates and hydrazide/ hydra zones: Anti – Mycobacterium tuberculosis activity and cytotoxicity, *Eur. J. Med. Chem*., **2010**, 45, 1898-1905.
[11]. F. A. French, E. J. Blanz, Jr, J. R. DoAmaral, D. A. French,Carcinostatic activity of thiosemi carbazones of formyl heteroaromatic Compounds, VI. 1-Formylisoquinoline Derivatives bearing additional Ring substitutions, with Notes on Mechanism of Action, *J. Med. Chem*.,**1970**, 13, 1117-1124.
[12]. N. J. Beasley, R. Prevo, S. Banerji, R. D. Leek, J. Moore, P. van Trappen, Intratumoral lymphangiogenesis and lymph node metastasis in head and neck cancer, *Cancer. Res.*, **2002**, 62, 1315-1320.
[13]. J. L. Su, C. J. Yen, P. S. Chen, S. E. Chuang, C. C. Hong, I. H. Kuo, The role of the VEGF-C/VEGFR-3 axis in cancer progression, *Br. J. Cancer*., **2007**, 96, 541-545.

[14]. N. Simiantonaki, C. Jayasinghe, R. Michel-Schmidt, K. Peters, M.I. Hermanns, C. J. Kirkpatrick, Hypoxia-induced epithelial VEGF-C/VEGFR-3 upregulation in carcinoma cell lines, *Int. J. Oncol.,* **2008**, 32, 585-592.
[15]. Y. He, T. Karpanen, K. Alitalo, Role of lymphangiogenic factors in tumor metastasis. *Biochim. Biophys. Acta*., **2004**, 1654, 3-12.
[16]. B. N. Figgi's, J. Lewis, Modern coordination chemistry, Ed. J. Lewis, R.C. Wilkinson, Wiley interscience, New York, **1967**.
[17]. J. Marmur, A procedure for isolation of deoxyribonucleic acid from micro-organisms, *J. Mol. Biol.,* **1961**, 3, 208-218.
[18]. M. E. Reichmann, S. A. Rice, C. A. Thomas, P. Doty, A further examination of the molecular weight and size of desoxypentose nucleic acid, *J. Am. Chem. Soc.*, **1954**, 76, 3047-3053.
[19]. F. Garland, D. E. Graves, L.W. Yielding, H. C. Cheung, Comparative studies of the binding of ethedium bromide and its photo reactive analogues to nucleic acids by fluorescence and kinetics, *Biochemistry*., **1980**, 19, 3221-3226.
[20]. A. Wolfe, G. H. Shimer Jr, T. Meehan, Polycyclic aromatic hydrocarbons physically intercalate into duplex regions of denatured DNA, *Biochemistry*, **1987**, 26, 6392-6396.
[21]. K. Hostettman, J. L. Wolfender, S. Rodriguez, Rapid detection and subsequent isolation of bioactive constituents of crude plant extracts, *Planta. Med.,* **1997**, 63, 2-10.
[22]. F. Hadacek, H. Greger, Testing of antifungal natural products: Methodologies, comparability of results and assay choice, *Phytochem. Anal.,* **2000**, 11, 137-147.
[23]. L. Yan, L. Han, L. Zhihai, R. Wang, Comparative assessment of scoring functions on an updated benchmark: 2. Evaluation methods and general results, *J. Chem. Inf. Model.,* **2014**, 54, 1717-1736.
[24]. K. Nakamoto, In: Nakamoto (ed) Infrared and Raman spectra of inorganic and coordination compounds, third edn. John Wiley & sons, New York, **1978**.
[25]. P. M. Krishna, K. H. Reddy, J. P. Pandey, D. Siddavattam, Synthesis, Characterization, DNA binding and nuclease activity of binuclear Cu (II) complexes of cuminaldehydethiosemi carbazones, *Transition Met. Chem.*, **2008**, 33, 661-668.
[26]. A. C. Massabni, P. P. Corbi, P. Melnikov, M. A. Zacharias, H. R. Rechenberg, Four new metal complexes with the amino acid deoxyalliin, *J. Braz. Chem. Soc.,***2005**, 16, 718-722.
[27]. K. P. Chennam, M. ravi, B. Ushaiah, V. Srinu, R.K. Eslavath, Ch. S. Devi, Synthesis, characterization, DNA interactions, DNA cleavage, radical scavenging activity, antibacterial, anti-proliferative and docking studies of new transition metal complexes, *J. fluoresc.*, **2016**, 26, 189-205.
[28]. Z. Tian, Y. Huang, Y. Zhang, L. Song, Y. Qiao, X. Xu, C. Wang, Spectroscopic and molecular modeling methods to study the interaction between naphthalimide-polyamine conjugates and DNA,*J. Photochem. Photobiol. B. Biology.,* **2016**, 158, 1-15.
[29]. S.M Mohamadi, Y. Ebrahimipour, J. Castro, M. Torkuzadeh-Mahani, Synthesis, characterization, crystal structure, DNA and BSA binding, molecular docking and in vitro anticancer activities of a mononuclear dioxide-uranium (VI) complex derived from a tridentate ONO aroylhydrazone, *J. Photochem. Photobiol. B. Biology*., **2016**, 158, 219-227.
[30]. V. Uma, M. Kanthimathi, T. Weyhermuller, B. U. Nair, Oxidative DNA cleavage mediated by new Cu(II) terpyridine complex: Crystal structure and DNA binding studies, *J. Inorg. Biochem.*, **2005**, 99, 2299-2307.
[31]. P. R. Reddy, A. Shilpa, Synthesis, characterization and DNA binding and DNA cleavage properties of dinuclear Cu^{II}-salophen/salen complexes, *Chem. Biodivers*., **2011**, 8, 1245-1265.
[32]. S. Satyanarayana, J. C. Dabrowiak, J. B. Chaires, Tris(phenanthroline)ruthenium(II) enantiomer interactions with DNA: Mode and specificity of binding, *Biochemistry.,***1993**, 32, 2573-2584.
[33]. D.D. Qin, Z.Y. Yang, B.D. Wang, Spectra and DNA-binding affinities of Copper(II), Nickel(II) complexes with a novel glycine Schiff base derived from chromone, *Spectrochim. Acta, Part A.*, **2007**, 68, 912-915.

[34]. A. K. Sharma, S. Chandra, Complexation of nitrogen and sulphur donor schiff's base ligand to Cr (III) and Ni (II) metal ions: Synthesis, spectroscopic and antipathogenic studies, *Spectrochim. Acta. A.*, **2011**, 78, 337-342.
[35]. G. Psomas, A. Tarushi, E.K. Eftimiadou, Y. Sanakis, C.P. Raptopoulou, N. Katsaros, Synthesis, structure and biological activity of copper(II) complexes with oxolinic acid, *J. Inorg. Biochem.***2006**, 100, 1764-1773.